Article

SOURCE DATA | TRANSPARENT PROCESS

EMBO reports

GAPDH facilitates homologous recombination repair by stabilizing RAD51 in an HDAC1-dependent manner

Munan Shi[1], Jiajia Hou[1], Weichu Liang[1], Qianwen Li[2], Shan Shao[1], Shusheng Ci[1,3], Chuanjun Shu[4], Xingqi Zhao[1], Shanmeizi Zhao[1], Miaoling Huang[1], Congye Wu[5], Zhigang Hu[1], Lingfeng He[1], Zhigang Guo[1,*] & Feiyan Pan[1,**]

Abstract

Homologous recombination (HR), a form of error-free DNA double-strand break (DSB) repair, is important for the maintenance of genomic integrity. Here, we identify a moonlighting protein, glyceraldehyde-3-phosphate dehydrogenase (GAPDH), as a regulator of HR repair, which is mediated through HDAC1-dependent regulation of RAD51 stability. Mechanistically, in response to DSBs, Src signaling is activated and mediates GAPDH nuclear translocation. Then, GAPDH directly binds with HDAC1, releasing it from its suppressor. Subsequently, activated HDAC1 deacetylates RAD51 and prevents it from undergoing proteasomal degradation. GAPDH knockdown decreases RAD51 protein levels and inhibits HR, which is re-established by overexpression of HDAC1 but not SIRT1. Notably, K40 is an important acetylation site of RAD51, which facilitates stability maintenance. Collectively, our findings provide new insights into the importance of GAPDH in HR repair, in addition to its glycolytic activity, and they show that GAPDH stabilizes RAD51 by interacting with HDAC1 and promoting HDAC1 deacetylation of RAD51.

Keywords GAPDH; HDAC1; homologous recombination; protein stability; RAD51

Subject Categories DNA Replication, Recombination & Repair; Post-translational Modifications & Proteolysis; Signal Transduction

DOI 10.15252/embr.202256437 | Received 7 November 2022 | Revised 23 May 2023 | Accepted 25 May 2023

EMBO Reports (2023) e56437

Introduction

The integrity and stability of DNA are critical for organism survival. DNA is continuously subjected to damage inflicted by environmental and endogenous insults (Chen *et al*, 2018). Among the most serious and lethal forms of DNA damage are double-strand breaks (DSBs), which are caused by exogenous agents such as ionizing radiation (IR) and certain chemotherapeutic drugs or by endogenous stresses, such as DNA replication errors and reactive oxygen species (ROS; Srinivas *et al*, 2019). When not repaired in a timely fashion, DSBs can induce cytotoxicity that destabilizes the genome, leading to cell death or to mutations that promote carcinogenesis (Li & Heyer, 2008; Ciccia & Elledge, 2010).

Double-strand break repair is achieved through two main pathways: homologous recombination (HR) and nonhomologous end joining (NHEJ). NHEJ can occur throughout the cell cycle and can produce DNA with errors, while HR is an error-free process but requires a sister chromatid as a template and, therefore, HR only occurs during the late S/G2 phase of the cell cycle (Clarke *et al*, 2017). In addition to repairing DSBs, HR plays a prominent role in faithfully duplicating the genome by providing critical support for DNA replication and telomere maintenance (Li & Heyer, 2008). The core mechanistic steps of HR consist of joint molecule formation and strand exchange between DNA molecules, which are governed by multiple proteins, such as ATM, the MRE11–RAD50–NBS1 complex, BRCA1/2, and RAD51 (San Filippo *et al*, 2008; Sanchez-Bailon *et al*, 2021). Multiple regulatory mechanisms have evolved to ensure that HR takes place at the right time, place, and manner. Several of these previous studies have focused on the formation of Rad51 nucleofilaments, which play a central role in HR (Krejci *et al*, 2012). Although many mediators have been suggested to be involved in HR regulation, much of the concerted molecular events that underlie the HR process remain to be understood.

Glyceraldehyde-3-phosphate dehydrogenase (GAPDH), a key enzyme in glycolysis, has long been used as an internal control for the standardization of cytoplasmic protein expression because of its

1 Jiangsu Key Laboratory for Molecular and Medical Biotechnology, College of Life Sciences, Nanjing Normal University, Nanjing, China
2 Department of Radiotherapy, Taikang Xianlin Drum Tower Hospital, Nanjing University, Nanjing, China
3 School of Basic Medical Sciences, Nanjing Medical University, Nanjing, China
4 Department of Bioinformatics, School of Biomedical Engineering and Informatics, Nanjing Medical University, Nanjing, China
5 Department of Oncology, Nanjing First Hospital, Nanjing Medical University, Nanjing, China
*Corresponding author. Tel: +86 25 85891050; E-mail: guo@njnu.edu.cn
**Corresponding author. Tel: +86 25 85891050; E-mail: panfeiyan@njnu.edu.cn

constant expression in cells and tissues (Wu *et al*, 2012). Recently, several lines of evidence have indicated that the intracellular distribution of GAPDH changes in the presence of various stimuli, and GAPDH is called a moonlighting protein because of its multiple functions in transfer RNA (tRNA) nuclear transport, mRNA stabilization, inflammation, extracellular vesicles assembly, cell apoptosis, and autophagy (Sawa *et al*, 1997; Hara *et al*, 2005; Harada *et al*, 2007; Zeng *et al*, 2014; Chang *et al*, 2015; Kornberg *et al*, 2018; Galvan-Pena *et al*, 2019; Dar *et al*, 2021). Notably, GAPDH has been shown to play an important role in base excision repair (BER). GAPDH can bind DNA and recognize AP sites, enabling GAPDH participation in DNA repair (Sawa *et al*, 1997; Kosova *et al*, 2015). GAPDH also catalyzes the reduction of AP site endonuclease 1 (APE1) in an oxidation state, stimulates APE1 endonuclease activity, and facilitates BER (Azam *et al*, 2008; Hou *et al*, 2017). In addition, GAPDH binds to poly (ADP-ribose) polymerase (PARP1) to promote its activation under oxidative stress conditions (Nakajima *et al*, 2015). Our previous study revealed that upon methyl methanesulfonate (MMS) stimulation, GAPDH is phosphorylated by Src kinase and is translocated into the nucleus; where it directly interacts with DNA polymerase β (Polβ) to promote its polymerase, improving BER efficiency (Ci *et al*, 2020). All of the explanations described to date clearly demonstrate that GAPDH is involved in single-strand break (SSB) repair; however, whether GAPDH functions in the DSB repair is still unknown.

In this study, we found that GAPDH participates in HR by competitively binding with HDAC1 to enhance its activity, which in turn regulates RAD51 acetylation levels. We further demonstrate that RAD51 K40 deacetylation prevents its ubiquitination-based degradation, leading to sufficient RAD51 stable protein to enhance HR repair.

Results

IR induces GAPDH nuclear translocation

To investigate whether GAPDH responds to DSB repair, we treated a human cervical cancer cell line (HeLa), a proximal tubule cell line (HK2), and a bronchial epithelial cell line (BEAS-2B) with the DSB inducers etoposide (ETO), adriamycin (ADR), and ionizing radiation (IR) and examined the cellular distribution of GAPDH. All treatments induced GAPDH nuclear translocation (Figs 1A and EV1A). Western blot analysis of cytoplasmic and nuclear proteins confirmed this result (Fig 1B). After confirming GAPDH nuclear translocation upon DSB, we next wondered whether this process is mediated by Src signaling because our previous work revealed that Src signaling was activated and critical for GAPDH nuclear translocation after DNA SSB induction (Ci *et al*, 2020). We examined the phosphorylation level of Src Tyr529, an activation site that leads to inhibitory effects, and found that Tyr529 phosphorylation was remarkably reduced after IR exposure, indicating Src activation (Fig 1C). Next, the Src-specific inhibitor PP2 prevented IR-induced GAPDH nuclear translocation, supporting the importance of Src signaling in this process (Fig 1D). Notably, mutation of important sites involved with GAPDH nuclear translocation, namely Y41F (mutation in response to SSB not entering the nucleus; Ci *et al*, 2020), S122A (mutation that does not enter the nucleus under starvation), S122D (nuclear localization mutation; Chang *et al*, 2015) or C152S (glycolytic activity dead mutation; Chakravarti *et al*, 2010), did not change GAPDH nuclear location, compared with that of the wild type (WT), after IR exposure (Fig EV1B–D), suggesting that sites other than those mutated are critical for DSB-induced nuclear import of GAPDH.

To investigate whether GAPDH participates in DNA repair, we examined its interaction with γH2AX, a well-established DSB marker. Immunoprecipitation assays revealed that endogenous GAPDH could be coprecipitated with γH2AX under various DSB-inducing treatments (Figs 1E and F, and EV1E and F). These results suggest that GAPDH may play a role in the repair of DSB.

GAPDH is involved in DSB repair

To assess the role of GAPDH in DSB repair, three distinct siRNA sequences were designed to knock down GAPDH expression, and the knockdown efficiency of these siRNAs was verified by western blotting (Fig 2A). GAPDH knockdown significantly decreased cell survival after ADR and IR treatment (Figs 2B and EV2A). Immunofluorescence staining of γH2AX and 53BP1 revealed that GAPDH knockdown cells exhibited an increase in γH2AX foci and 53BP1 foci, indicating the accumulation of DNA damage (Figs 2C and D, and EV2B). Additionally, the neutral comet assay and alkaline comet assay in stable GAPDH knockdown HeLa cells revealed that DNA damage persisted after GAPDH knockdown (Figs 2E and EV2C and D). Considering that abnormal metabolism is closely linked to ROS (Martinez-Reyes & Chandel, 2021), we examined intracellular ROS levels, which showed no difference between control and GAPDH-deficient HeLa cells, excluding the possibility of ROS-induced DNA damage (Fig EV2E). Altogether, these data verified that GAPDH is essential for DSB repair.

To determine whether GAPDH participates in DSB repair, we examined the γH2AX level at different time points after IR treatment. In control cells, the γH2AX level increased until the 4-h time point and gradually declined until the 24-h time point (Fig 2F). However, GAPDH knockdown cells exhibited significantly higher γH2AX levels at all time points, indicating a deficiency in DSB repair (Fig 2F). We next applied DR-GFP and EJ5-GFP reporter systems to evaluate HR and NHEJ efficiency. Our results showed that GAPDH knockdown decreased HR efficiency by approximately 30% (Fig 2G) while also reducing the percentage of cells in the S phase by approximately 10% (Figs 2H and EV2F), suggesting that beyond the cell cycle, other factors are involved in the observed 30% reduction in HR repair efficiency upon GAPDH knockdown. The efficiency of NHEJ was similarly decreased to that of HR (Fig EV2G). These findings suggest that GAPDH is involved in both HR and NHEJ pathways and plays a crucial role in DSB repair.

To investigate whether GAPDH effects in DSB repair depend on its enzymatic activity, we analyzed the enzymatic activity of GAPDH in HeLa cells before and after IR treatment. We found it was markedly reduced after IR treatment (Fig 2I). Next, pretreatment with heptelidic acid (HA), a specific GAPDH inhibitor of its enzymatic activity (Liberti *et al*, 2017), exacerbated IR-induced DNA damage and induced G1 phase arrest (Fig EV2H and I), suggesting that GAPDH participation in DSB repair is closely related to its enzymatic activity. Collectively, these data indicated that GAPDH is involved in DSB repair.

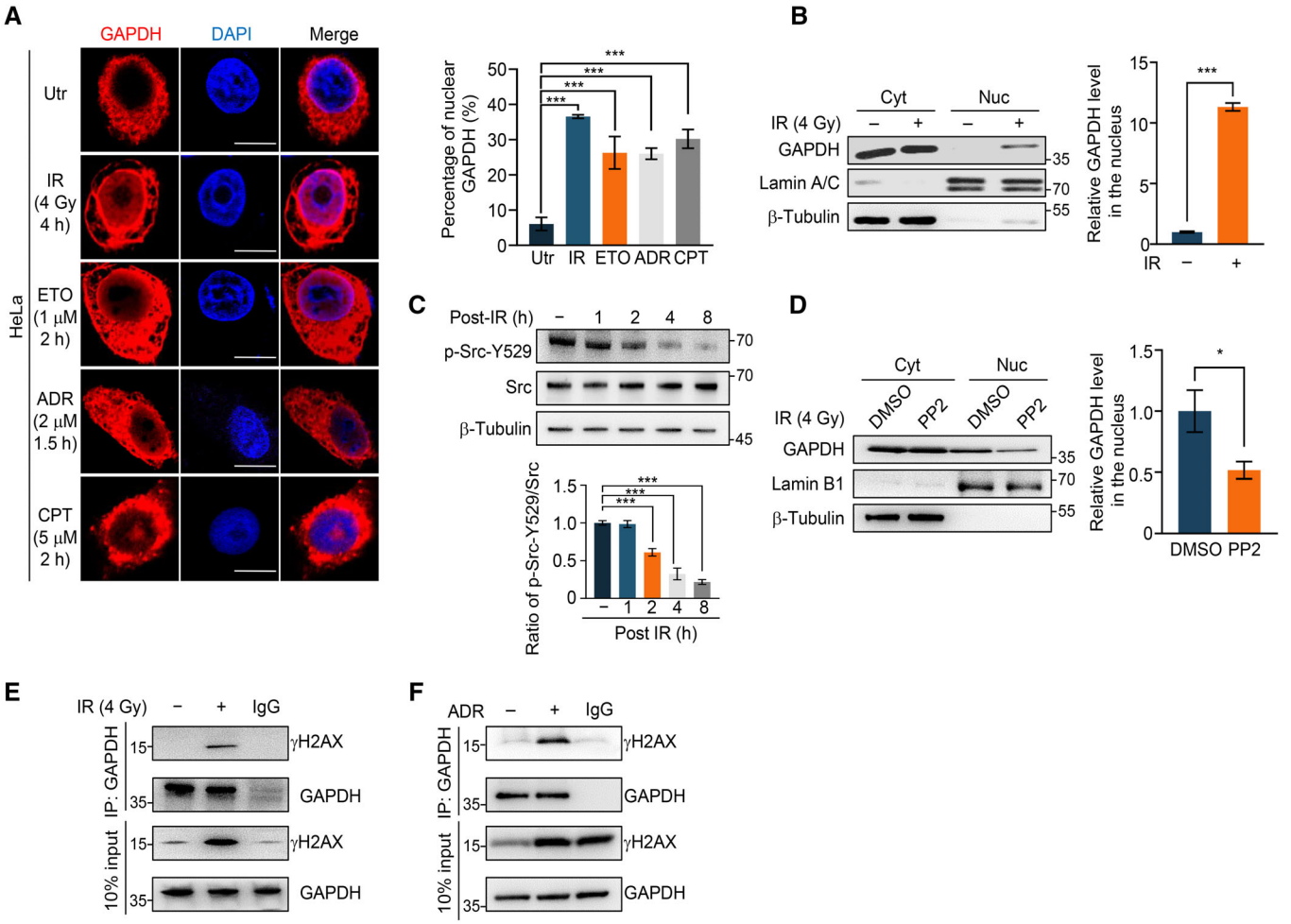

Figure 1. DSBs induced GAPDH nuclear translocation via Src signaling.

A Representative immunofluorescence images (left) of GAPDH (red) in HeLa cells untreated (Utr), or treated with IR, etoposide (ETO), adriamycin (ADR), and camptothecin (CPT) as indicated. DNA was stained with DAPI (blue). Quantitative analysis (right) of nuclear GAPDH. Scale bars, 10 μm.

B Immunoblot (left) and quantification (right) of endogenous GAPDH in subcellular fractions of HeLa cells treated 4 Gy IR and recovered for 4 h. β-Tubulin and Lamin A/C served as indicators for the cytoplasmic and nuclear fractions.

C Immunoblot (upper) and quantification (lower) of phospho-Src-Y529 in HeLa cells collected at the indicated time points after 4 Gy IR treatment.

D HeLa cells were pretreated with or without 10 μM PP2 for 24 h and exposed to 4 Gy IR. After 4 h of recovery, nuclear and cytoplasmic fractions were separated and subjected to immunoblot with indicated antibodies (left). Quantification of nuclear GAPDH is in the right panel. β-Tubulin and Lamin B1 served as indicators for the cytoplasmic and nuclear fractions.

E, F Immunoblot of anti-GAPDH immunoprecipitates from HEK293T treated with 4 Gy IR and recovered for 4 h (E), or with 5 μM ADR for 2 h (F).

Data information: Data represented as mean ± s.d. of at least three independent experiments. *P*-values are from Student's *t*-tests. *$P < 0.05$; ***$P < 0.001$ (A–D).
Source data are available online for this figure.

GAPDH regulates RAD51 protein stability

Homologous recombination is the major DSB repair pathway that maintains genome integrity. To explore the intrinsic mechanism of GAPDH function in DSB repair, particularly in HR, the expression levels of HR-related proteins were examined, and RAD51 was found to be significantly decreased after GAPDH knockdown (Fig 3A). Notably, in GAPDH knockdown HeLa cells, the ionizing radiation-induced foci (IRIF) resolution of RAD51 and γH2AX was delayed (Figs 3B and EV3A), suggesting that the loss of GAPDH impairs DNA repair. Furthermore, GAPDH knockdown markedly decreased RAD51 foci in the S phase, as determined by immunofluorescence double staining of RAD51 and Cyclin A (Fig EV3B), confirming a role of GAPDH in HR, in addition to its function in the cell cycle.

Although GAPDH can stabilize mRNA (Zeng *et al*, 2014), qPCR analysis showed that the reduction in RAD51 expression levels was not due to mRNA level changes (Fig 3C). Overexpression of GAPDH increased RAD51 protein levels (Fig 3D) and restored GAPDH knockdown-reduced RAD51 levels (Figs 3E and EV3C). Next, RAD51 protein levels in HeLa cells with or without GAPDH knockdown were examined at different time points in the presence of the protein synthesis inhibitor cycloheximide (CHX). In contrast to the control group, GAPDH knockdown significantly decreased RAD51

protein stability (Fig 3F). Moreover, as RAD51 was degraded via the proteasomal pathway (Inano *et al*, 2017), pretreatment with the proteasome inhibitor MG132 completely reversed the GAPDH deficiency-induced decrease in RAD51 protein levels (Figs 3G and EV3C), confirming the modulation of RAD51 protein stability by GAPDH. Additionally, HA treatment did not change the RAD51 protein level, suggesting that HA-induced modulation occurred dependent on GAPDH activity (Fig EV3D). Together, these results demonstrate that GAPDH responds to DNA damage by regulating RAD51 levels.

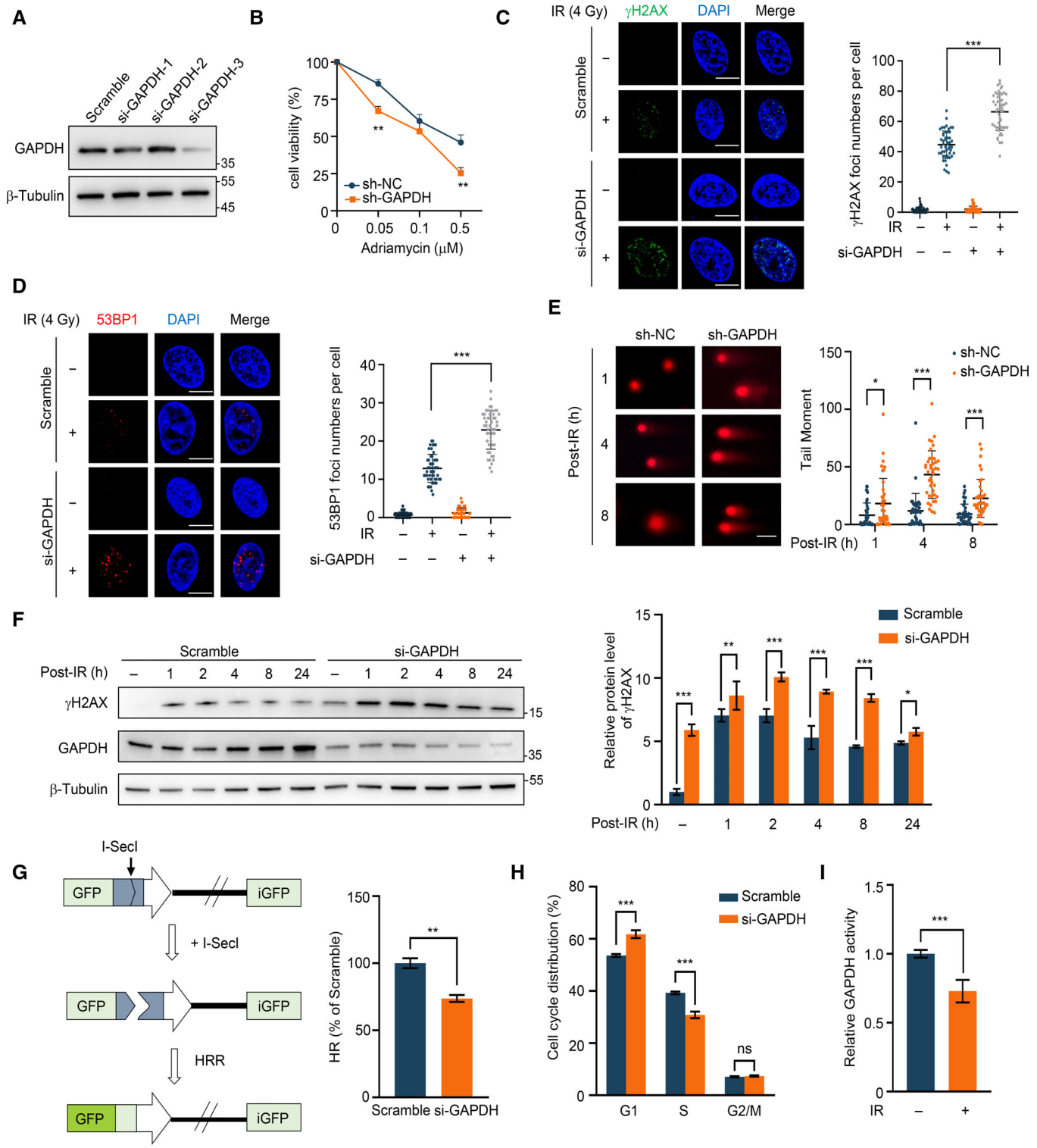

Figure 2.

Figure 2. GAPDH is essential for homologous recombination repair.

A Immunoblot of GAPDH in whole cell lysates of HeLa cells transfected with scramble siRNA and three different si-GAPDH for 48 h. The following experiments utilized the si-GAPDH-3 sequence to knock down GAPDH.

B Cell viability analysis of HeLa cells stably expressing the sh-NC and sh-GAPDH were treated with the indicated concentration of ADR for 48 h.

C, D Left, representative immunofluorescence images of γH2AX (C, green) or 53BP1 (D, red) in HeLa cells transfected with scramble siRNA or si-GAPDH after 4 Gy IR exposure and recovered for 4 h. DNA was stained with DAPI (blue). Right, quantification of γH2AX or 53BP1 foci/cell ($n = 50$). Mann–Whitney *U*-test. Scale bars, 10 μm.

E Neutral comet assay (left) and quantification of the tail moment (right) showing the tail moment of stable GAPDH knockdown HeLa cells ($n = 40$) and control cells ($n = 40$) under IR treatment and recovered for the indicated time. Mann–Whitney *U*-test. Scale bar, 100 μm.

F Immunoblot (left) and quantification (right) of γH2AX in HeLa cells pretransfected with scrambled siRNA or si-GAPDH and recovered at indicated points after 4 Gy IR exposure.

G Left, schematic diagram of HR reporter system. Right, analysis of HR repair activity in U2OS cells treated with scrambled siRNA and si-GAPDH.

H Cell cycle analysis of HeLa cells transfected with scramble siRNA or si-GAPDH.

I GAPDH activity in HeLa cells treated with or without 4 Gy IR and recovered for 4 h.

Data information: Data represented as mean ± s.d. of at least three independent experiments. *P*-values are from Student's *t*-tests. $^{*}P < 0.05$; $^{**}P < 0.01$; $^{***}P < 0.001$; ns: not significant (B–I).
Source data are available online for this figure.

Acetylation-mediated proteasomal degradation is critical for the regulation of RAD51 by GAPDH

Acetylation, a post-translational modification, plays a critical role in protein stability, enzymatic activity, and DNA binding (Verdin & Ott, 2015). Reduction in RAD51 protein levels has been detected after treatment with deacetylase inhibitors such as valproic acid (VPA) and trichostatin A (TSA; Romeo *et al*, 2022). However, whether and how RAD51 is acetylated is entirely unknown. In this study, we first confirmed that RAD51 expression was decreased by treatment with the deacetylase inhibitor TSA (Fig 4A), and we found that this decrease was due to loss of protein stability but not transcriptional regulation (Figs 4B and EV4A). To evaluate the relationship between RAD51 acetylation and proteasomal degradation, we pretreated HeLa cells with MG132 and then examined RAD51 acetylation by IP-western blot analysis. The results clearly illustrated that RAD51 was acetylated and that the acetylation of RAD51 was enhanced by GAPDH knockdown (Fig 4C). Interestingly, in the absence of MG132 treatment, GAPDH deficiency led to a decrease in RAD51 acetylation levels (Fig EV4B), suggesting that GAPDH may be involved in regulating RAD51 protein stability by modulating its acetylation status. Next, we acetylated purified RAD51 *in vitro* using HeLa whole cell lysate as an acetylase donor and then performed a mass spectrometry analysis to explore the specific acetylation sites (Fig EV4C and D). We successfully identified five acetylated sites (Fig 4D and Dataset EV1). To elucidate the effect of acetylating these sites on RAD51, we constructed five RAD51 deacetylation-mimetic mutants (Lys residues replaced with Arg residues) as follows: K40R, K64R, K70R, K80R, and K285R. Compared with WT and other mutants, the expression of the K40R RAD51 mutant was significantly increased (Fig 4E). Multiple sequence alignment revealed that Lys40 was highly conserved among species (Fig 4F). To assess the importance of K40 acetylation, we then generated the RAD51 acetylation-mimetic mutant K40Q (a Lys residue replaced with a Glu residue). As anticipated, the expression level of the K40Q mutant was lower than that of WT or K40R RAD51 (Fig 4G). To explore the relationship between acetylation and ubiquitination, we overexpressed HA-ubiquitin with WT, K40R, and K40Q RAD51, and an IP-western blot analysis showed that the ubiquitination level of K40Q was much higher than that of WT or K40R RAD51 (Figs 4H and I, and EV4E and F), which indicated that Lys40 is the key acetylation site for ubiquitination of RAD51. Furthermore, RAD51 foci formation in response to IR was affected by Lys40 acetylation (Figs 4J and EV4G). Taken together, these results suggest that acetylation of Lys40 in RAD51 promotes RAD51 degradation via the ubiquitin-proteasome pathway.

GAPDH interacts with HDAC1 and promotes HDAC1 activity

Our previous mass spectrometry analysis identified histone deacetylase 1 (HDAC1) in the immunoprecipitates of GAPDH (Fig EV5A; Ci *et al*, 2020). The interaction between GAPDH and HDAC1 was confirmed by co-immunoprecipitation (co-IP; Fig 5A–C). The co-IP experiment with purified proteins further proved direct binding (Fig 5D). These results suggest a direct and specific interaction between GAPDH and HDAC1.

To determine the biological significance of the GAPDH and HDAC1 interaction, we first examined HDAC1 activity in HeLa cells with or without GAPDH knockdown. Notably, GAPDH knockdown significantly weakened HDAC1 activity (Fig 5E). This result was confirmed by the acetylation level of p53 and the expression level of p21, which were used to evaluate HDAC1 activity (Ito *et al*, 2002; Fig EV5B and C). Additionally, IR exposure decreased HDAC1 activity (Fig EV5D), which was consistent with the effect of p53 acetylation (Fig EV5B). HDAC1 activity was unexpectedly decreased after GAPDH overexpression (Fig EV5E), which may have been due to GAPDH-induced cell apoptosis (Nakajima *et al*, 2017). In contrast, GAPDH activity was increased by HDAC1 overexpression (Fig EV5F).

HDAC1 activity in cells is inhibited by the mammary serine protease inhibitor Maspin (Li *et al*, 2006; Shankar *et al*, 2020). To investigate whether Maspin affects GAPDH-regulated HDAC1 activity, we first examined Maspin protein levels before and after GAPDH knockdown, and no significant difference was observed (Fig EV5G). We then predicted the initial low-energy protein-to-protein docking complex structures of the three proteins by Vakser and ClusPro 2.0. HDAC1 bound with both GAPDH and Maspin, and importantly, HDAC1 formed a conflicting binding "pocket" with both proteins (Fig 5F). After confirming the interaction of HDAC1 and Maspin (Fig 5G and H), we examined the binding between GAPDH and HDAC1 and between HDAC1 and Maspin in cells after IR exposure. As predicted, IR treatment enhanced the interaction between

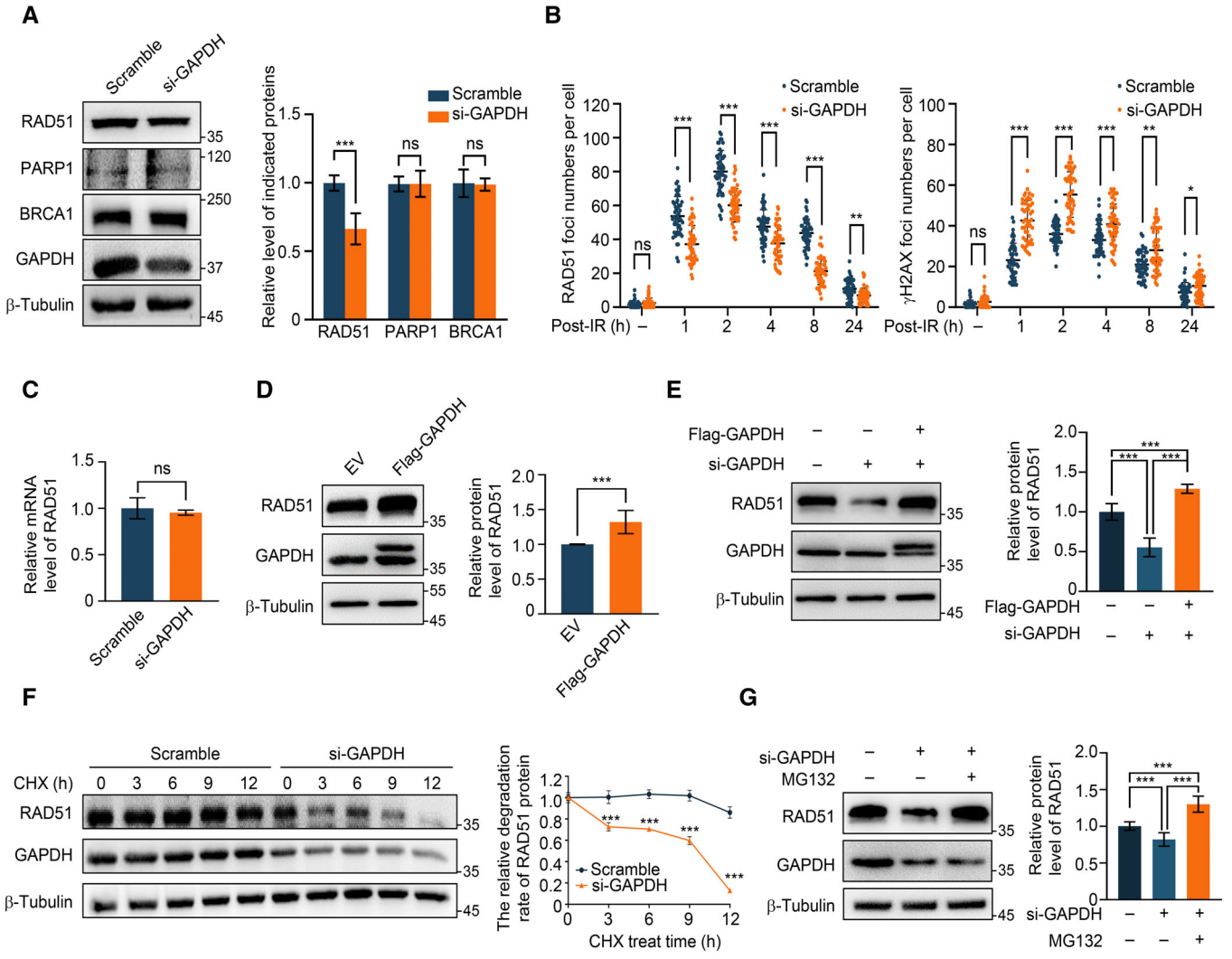

Figure 3. GAPDH regulates the protein stability of RAD51.

A Immunoblot (left) and quantification (right) of HR proteins in HeLa cells transfected with scrambled siRNA and si-GAPDH.

B Quantification of RAD51 (left) or γH2AX (right) foci/cell in HeLa cells pretransfected with scrambled siRNA or si-GAPDH, recovered at the indicated time points after 4 Gy IR exposure ($n = 50$). Mann–Whitney *U*-test.

C RT–qPCR analysis of RAD51 mRNA level in HeLa cells treated the same as (A).

D Immunoblot (left) and quantification (right) of RAD51 in HeLa cells with or without overexpression of GAPDH.

E Immunoblot (left) and quantification (right) of RAD51 in GAPDH knockdown HeLa cells reconstituted with Flag-GAPDH.

F Immunoblot (left) and quantification (right) of RAD51 in HeLa cells with or without GAPDH knockdown treated with 50 μg/ml CHX at the indicated time points.

G Immunoblot (left) and quantification (right) of RAD51 in GAPDH knockdown HeLa cells and control cells treated with or without MG132 (10 μM) for 10 h.

Data information: Data represented as mean ± s.d. of at least three independent experiments. *P*-values are from Student's *t*-tests. *$P < 0.05$; **$P < 0.01$; ***$P < 0.001$; ns, not significant (A–G).
Source data are available online for this figure.

GAPDH and HDAC1 while diminishing that between Maspin and HDAC1 (Fig 5I and J), suggesting that GAPDH promoted HDAC1 dissociation from Maspin. To identify the critical domain of HDAC1 for its interaction with GAPDH, we generated three different HDAC1 truncation mutants: HDAC1-S1 (N terminal with deacetylase domain), HDAC1-S2 (C terminal with nuclear localization signal), and HDAC1-S3 (depletion of amino acids 306–353, the segment predicted to mediate HDAC1 binding with GAPDH; Fig 5K). The ectopically expressed full-length HDAC1 and truncation mutants were pulled down by immunoprecipitation, and the result showed that GAPDH efficiently coprecipitated with the full-length HDAC1, HDAC1-S1, while not with HDAC1-S2 and HDAC1-S3, suggesting segment (306–353) of HDAC1 is important for its binding with GAPDH (Fig 5L). It is worth noting that the result of Maspin in the precipitates is consistent with GAPDH, indicating that the two proteins may bind to the same segment of HDAC1 (Fig 5L). After DSB occurs, GAPDH binds more to the full-length HDAC1 than to the undamaged state, while the binding of Maspin to full-length HDAC1

and HDAC1-S1 dramatically decrease. These further suggest the possibility that GAPDH competes with Maspin for binding to HDAC1 after DSB occurrence (Fig 5M). Interestingly, HDAC1-S1 did not exhibit increased binding to GAPDH as HDAC1-FL did after IR treatment, indicating that the nuclear localization signal (NLS) is also vital for the association of HDAC1 with GAPDH in response to DSBs (Fig EV5H). Furthermore, adding purified GAPDH to the nuclear lysate effectively increased HDAC1 activity *in vitro* (Figs 5N and EV5I), confirming the positive regulation of HDAC1 activity by nuclear GAPDH.

HDAC1 is the deacetylase of RAD51 and required for HR repair

We next asked whether HDAC1 activity regulates RAD51 protein levels. We overexpressed HDAC1-WT, HDAC1-S3 (Δ306–353), and HDAC1-H141A mutant (an enzymatic dead HDAC1; Mal *et al*, 2001) in HEK293T cells. HDAC1-S3 and HDAC1-H141A did not increase RAD51 protein levels as HDAC1-WT did (Fig 6A). Given that HDAC1 had no effect on the mRNA level of RAD51 (Appendix Fig S1A), we hypothesized that RAD51 may be a substrate for HDAC1. We found that endogenous RAD51 can interact with Flag-

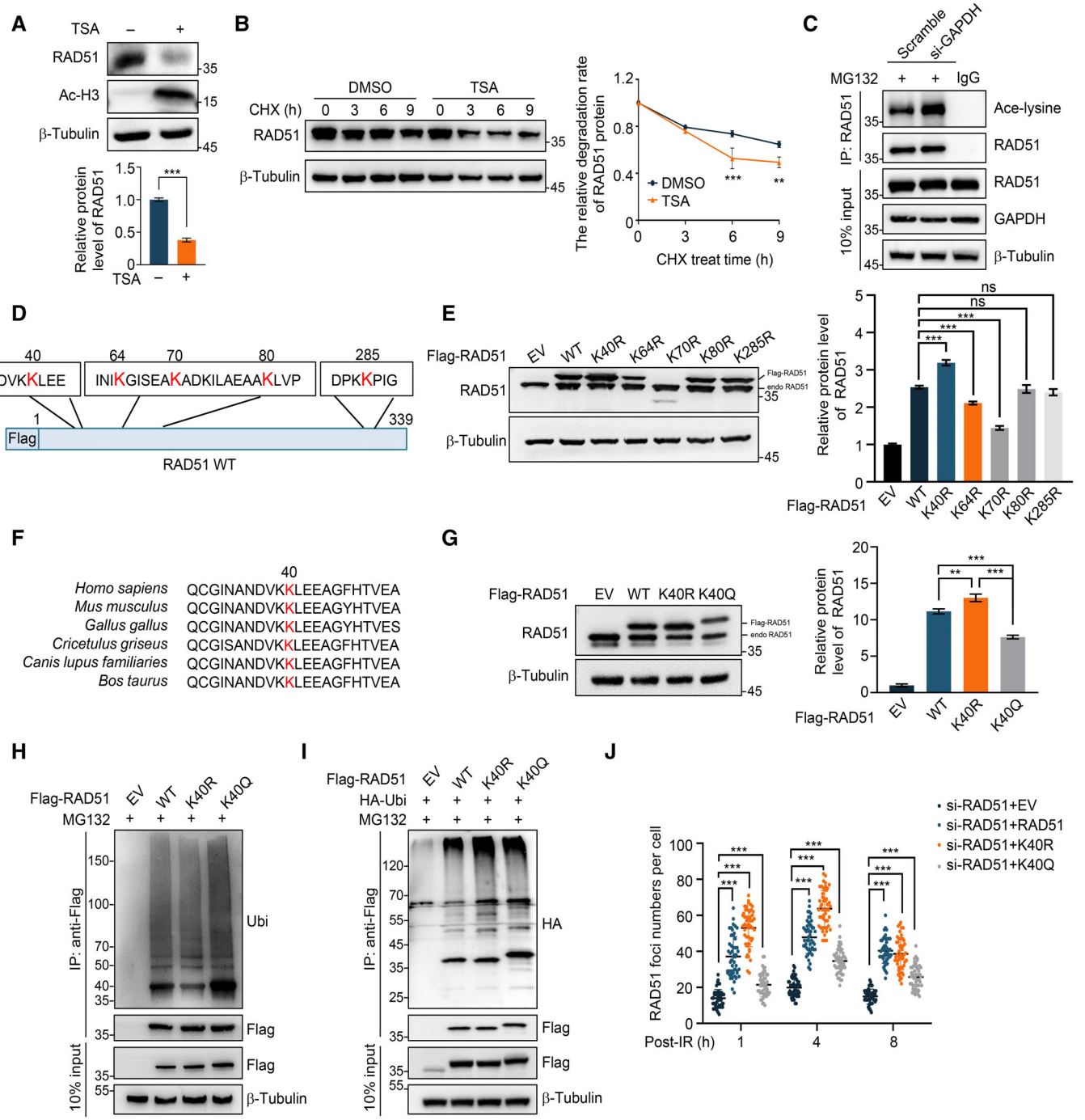

Figure 4.

Figure 4. Acetylate on K40 modulates RAD51 stability.

A Immunoblot (upper) and quantification (lower) of RAD51 in HeLa cells treated with or without 10 μM TSA for 24 h.
B Immunoblot (left) and quantification (right) of RAD51 in HeLa cells at different durations of 50 μg/ml CHX administration with or without TSA (10 μM, 12 h) treatment.
C Immunoblot of cell lysates or anti-RAD51 immunoprecipitates from HeLa cells with scramble siRNA or si-GAPDH transfection treated with MG132 (10 μM) for 2 h.
D Diagram showing the sequence of acetylation sites of RAD51.
E Immunoblot (left) and quantification (right) of Flag-RAD51 in cell lysates from HEK293T cells transfected with indicated Flag-RAD51 mutations. Endogenous RAD51 and Flag-RAD51 are denoted, respectively.
F Alignment of RAD51 amino acid sequence from different species.
G Immunoblot (left) and quantification (right) of Flag-RAD51 from HEK293T cells transfected with Flag-RAD51-WT, K40R, and K40Q. Endogenous RAD51 and Flag-RAD51 are denoted, respectively.
H Immunoblot of cell lysates or anti-Flag immunoprecipitates from HEK293T cells transfected with indicated Flag-RAD51 mutations and then exposed to 10 μM MG132.
I Immunoblot of cell lysates or anti-Flag immunoprecipitates from HEK293T cells transfected with HA-Ubiquitin and indicated Flag-RAD51 mutations and then exposed to 10 μM MG132.
J Quantifications of RAD51 foci/cell in HeLa cells transfected with si-RAD51 and indicated RAD51 mutations. Cells were exposed to 4 Gy IR and recovered at the indicated time (n = 50). Mann–Whitney U-test.

Data information: Data represented as mean ± s.d. of at least three independent experiments. P-values are from Student's t-tests. *P < 0.05; **P < 0.01; ***P < 0.001; ns, not significant (A, B, E, G, J).
Source data are available online for this figure.

HDAC1 as well as its enzymatically dead mutant H141A, but reduced acetylation levels of RAD51 occurred only in overexpressed HDAC1, not H141A (Fig 6B and C). This result suggests that HDAC1 can interact with and deacetylate RAD51.

To address whether HDAC1 mediates GAPDH function in HR repair, we first measured RAD51 expression in GAPDH knockdown HeLa cells, which was rescued by Flag-HDAC1 but not Flag-SIRT1 (Figs 6D and EV3C; Appendix Fig S1B). The number of RAD51 foci in GAPDH knockdown cells treated with IR was similarly rescued by Flag-HDAC1 (Fig 6E). In addition, HDAC1 overexpression successfully decreased GAPDH knockdown-induced γH2AX (Fig 6F and G), which confirmed that HDAC1 is the specific deacetylase mediating GAPDH-regulated RAD51 expression and DSB repair.

Discussion

Studies by our laboratory and others have demonstrated that GAPDH plays an important role in SSB repair (Kosova *et al*, 2015; Nakajima *et al*, 2015; Hou *et al*, 2017; Ci *et al*, 2020). In this study, we identified that GAPDH is translocated into the nucleus in response to DSBs and functions in DSB repair. Mechanistically, nuclear GAPDH interacts with and activates HDAC1, thus promoting RAD51 deacetylation and stabilizing RAD51 protein levels.

GAPDH serves not only as a key enzyme in glycolysis but also as a moonlighting protein involved in multiple biological processes, such as autophagy, telomere protection, nuclear export of tRNAs, and mRNA stability (Demarse *et al*, 2009; Kornberg *et al*, 2010). Recent evidence has revealed that GAPDH participates in SSB repair by binding to AP sites (Kosova *et al*, 2015) or directly interacting with APE1 (Azam *et al*, 2008) or Polβ (Ci *et al*, 2020) to promote BER. In this study, we found that GAPDH responds to DSBs and is translocated into the nucleus where it interacts with the DSB marker γH2AX, suggesting its involvement in DSB repair. The nuclear distribution of GAPDH is necessary for its DNA repair function; however, GAPDH lacks a nuclear localization signal (NLS). Post-translational modification has been implicated in its nuclear entry, and these modifications include S-nitrosylation by NO at Cys152 (Hara

Figure 5. GAPDH interacts with and promotes the activity of HDAC1.

A Immunoblot of HDAC1 in anti-GAPDH immunoprecipitates from HeLa cells.
B Immunoblot of GAPDH in anti-HDAC1 immunoprecipitates from HeLa cells.
C HeLa cells were transfected with or without Flag-GAPDH and HA-HDAC1 and then subjected to immunoprecipitation and immunoblots as indicated.
D Recombinant HDAC1 protein and recombinant GAPDH protein were co-incubated at 4°C for 2 h. *In vitro* immunoprecipitation was performed using anti-HDAC1 and subjected to immunoblots as indicated.
E Relative HDAC1 activity (left) in nuclear fractions from HeLa cells transfected with scrambled siRNA or si-GAPDH. Immunoblot (right) of GAPDH in nuclear fractions from HeLa cells.
F Steric view of HDAC1, GAPDH, and Maspin. HDAC1 and Maspin-specific binding domains are blue, and HDAC1 and GAPDH-specific binding domains are purple. Red indicates HDAC1 binding overlap region with Maspin and GAPDH.
G Immunoblot of HDAC1 in anti-Maspin immunoprecipitates from HeLa cells.
H Immunoblot of Maspin in anti-HDAC1 immunoprecipitates from HeLa cells.
I, J HeLa cells were treated with or without 4 Gy IR. The indicated cells were lysed for immunoprecipitation with anti-HDAC1 and immunoblotting analysis (left) for anti-Maspin (I) or anti-GAPDH (J). Quantitative analysis (right) of indicated protein levels.
K Schematic diagram depicting a set of Flag-HDAC1 expression constructs.
L, M Co-immunoprecipitation was performed to determine the interaction between endogenous GAPDH and Maspin, full-length Flag-HDAC1, and truncated forms of Flag-HDAC1 in HeLa cells, untreated (L) or treated with 4 Gy IR (M). Asterisks indicate nonspecific bands.
N Relative HDAC1 activity was measured by co-incubating 50 μg of nuclear extract with the corresponding mass of purified His-GAPDH protein for 15 min at 37°C.

Data information: Data represented as mean ± s.d. of at least three independent experiments. P-values are from Student's t-tests. *P < 0.05; **P < 0.01; ***P < 0.001 (E, I, J, N).
Source data are available online for this figure.

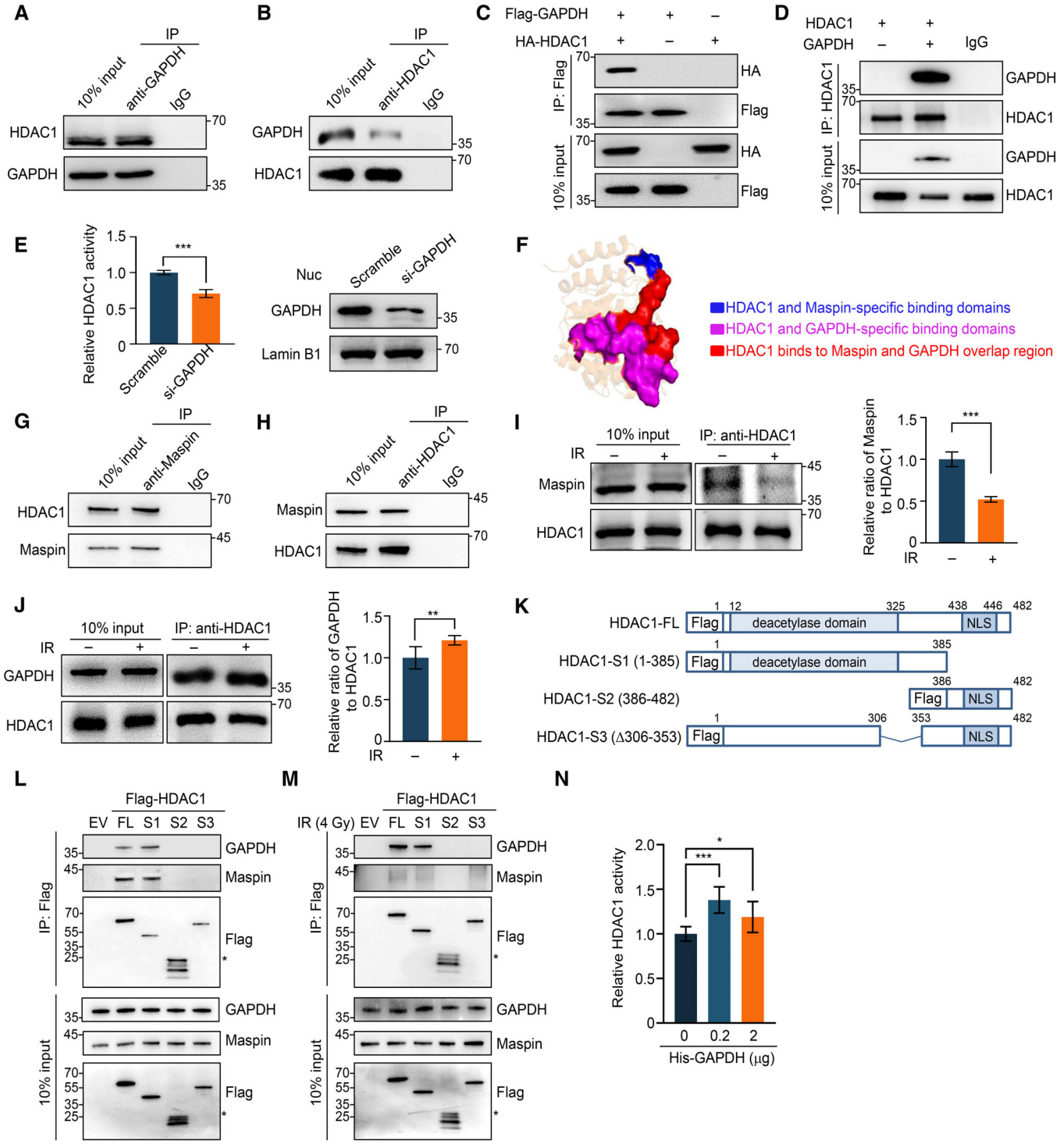

Figure 5.

et al, 2005), phosphorylation by AMPK at Ser122 (Chang *et al*, 2015), and phosphorylation by Src at Tyr41 (Ci *et al*, 2020). We generated GAPDH mutants to examine its nuclear distribution after IR stimulation and found that all of the mutated sites were not critical for GAPDH nuclear import, as indicated by no differences in the percentage of nuclear GAPDH in WT and the mutants. Notably, consistent with SSB-inducer treatment, Src signaling was highly activated and was necessary for GAPDH nuclear transport, as proven by treatment with the Src-specific inhibitor PP2. Our results imply that other amino acid sites play important roles in GAPDH nuclear translocation.

GAPDH is highly expressed in most cancers, which is related to the high demand for energy production through glycolysis (Zhu *et al*, 2021). In this study, we added another explanation: cancer

cells need GAPDH to meet their demands for DNA repair. Indeed, the enzymatic activity of GAPDH is important for DSB repair, and the decreased GAPDH activity after IR exposure suggests that cells may exhibit decreased glycolysis efficiency when repairing damaged DNA. However, when cells were pretreated with the GAPDH inhibitor HA, IR-induced DNA damage was profoundly exacerbated, suggesting the importance of GAPDH glycolytic activity for DNA repair. Interestingly, GAPDH can participate in the HR process, the

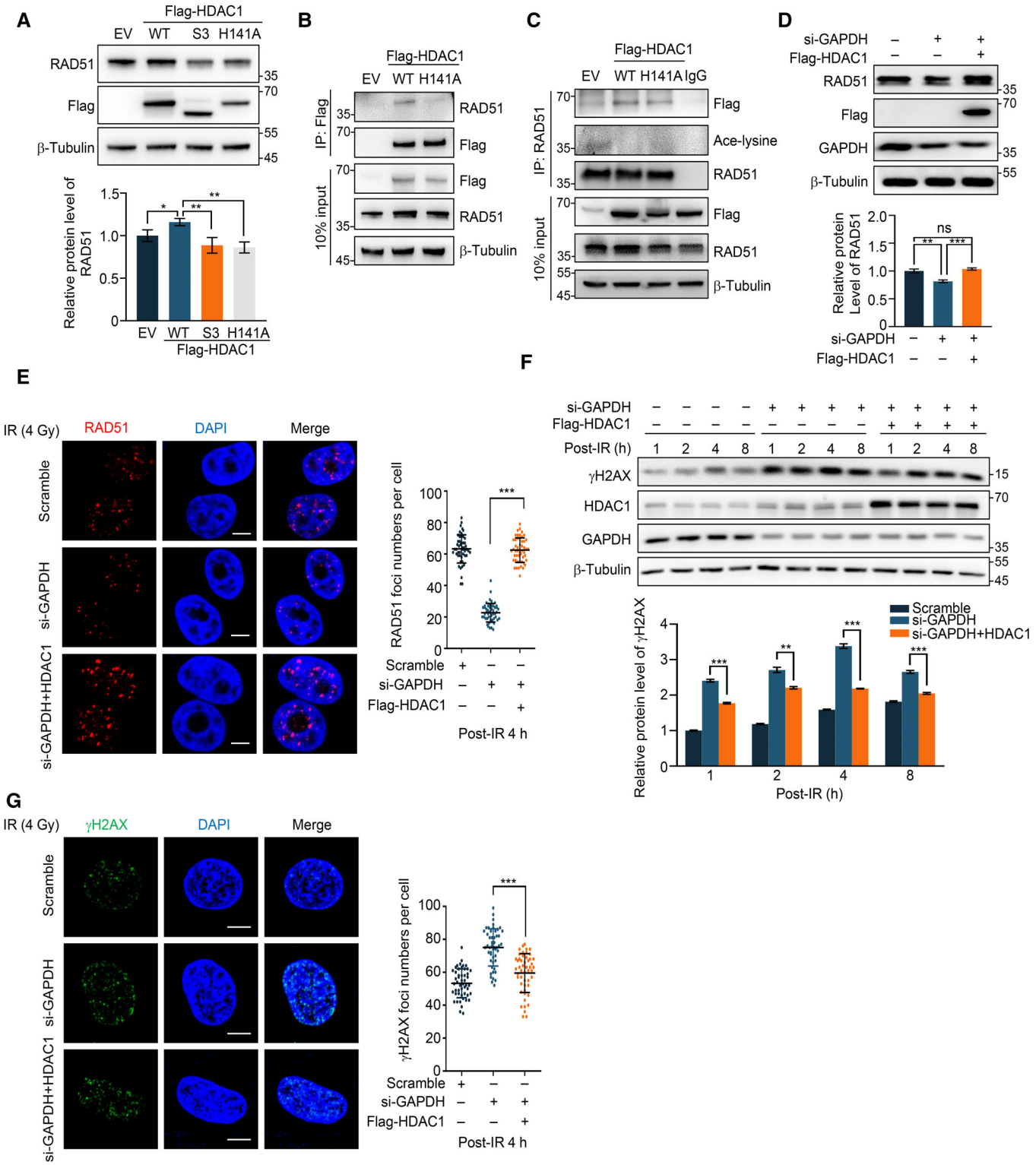

Figure 6.

Figure 6. HDAC1 deacetylates RAD51 and mediates GAPDH function in HR.

A Immunoblot (upper) and quantification (lower) of RAD51 in HEK293T cells transfected with empty vector, Flag-HDAC1, Flag-HDAC1-S3 (Δ306–353), and Flag-HDAC1-H141A.

B HeLa cells were transfected with empty vector, Flag-HDAC1, and Flag-HDAC1-H141A and then subjected to immunoprecipitation and immunoblots as indicated.

C HeLa cells were transfected with empty vector, Flag-HDAC1, and Flag-HDAC1-H141A and then subjected to immunoprecipitation and immunoblots as indicated.

D Immunoblot (upper) and quantification (lower) of RAD51 in GAPDH knockdown HeLa cells transfected with or without Flag-HDAC1.

E Left, GAPDH knockdown HeLa cells transfected with Flag-HDAC1 were treated with 4 Gy IR, fixed after 4 h, and immunostained with anti-RAD51 (red). DNA was stained with DAPI (blue). The number of RAD51 foci per cell is shown (right, $n = 50$). Mann–Whitney *U*-test. Scale bars, 5 μm.

F Immunoblot (upper) and quantification (lower) of γH2AX in GAPDH knockdown HeLa cells transfected with or without Flag-HDAC1 at the different time points after 4 Gy IR exposure.

G Left, GAPDH knockdown HeLa cells transfected with Flag-HDAC1 were treated with 4 Gy IR, fixed after 4 h, and immunostained with anti-γH2AX (green). DNA was stained with DAPI (blue). The number of γH2AX foci per cell is shown (right, $n = 50$). Mann–Whitney *U*-test. Scale bars, 5 μm.

Data information: Data represented as mean ± s.d. of at least three independent experiments. *P*-values are from Student's *t*-tests. $*P < 0.05$; $**P < 0.01$; $***P < 0.001$; ns, not significant (A, D–G).
Source data are available online for this figure.

main pathway of DSB, independent of its glycolytic activity. HA treatment did not exhibit the same effect on RAD51 expression as GAPDH knockdown, which demonstrates that RAD51 downregulation was not due to GAPDH activity.

We found that GAPDH plays an important role in DSB repair and that GAPDH deficiency resulted in increased accumulation of DNA damage in cells. Immunofluorescence staining showed that the number of γH2AX and 53BP1 foci was significantly higher in GAPDH knockdown cells than in control cells. The longer comet tail also indicated that the loss of GAPDH exacerbated the accumulation of intracellular DSBs. DSBs are mainly repaired in two ways, HR and NHEJ. We evaluated the repair efficiency of the two pathways by using classical reporter systems and found that the activation of both pathways was significantly decreased after GAPDH knockdown. HR is the pathway of DSB repair that maintains genomic stability, and HR efficiency is highly related to the cell cycle (Hustedt & Durocher, 2016). Our data showed that the cell cycle was arrested by GAPDH knockdown, which was consistent with a previous study (Phadke *et al*, 2009). Importantly, the decrease in the proportion of cells in the S phase was much less pronounced than the decrease in HR efficiency, indicating that the cell cycle was not fully responsible for the decline in HR efficiency. Therefore, GAPDH knockdown-reduced HR may be caused by two effects: a decrease in the proportion of cells in the S phase and decreased RAD51 protein levels. Cell cycle arrest by HA treatment verified that GAPDH glycolytic activity was essential for the cell cycle-dependent regulation of HR. We also noticed that NHEJ, which occurs throughout the whole cell cycle, was dramatically suppressed by GAPDH deficiency. Indeed, the decrease in the number of 53BP1 foci (Fig 2D) was indicative of NHEJ impairment because this well-known DSB marker is mainly expressed during NHEJ repair (Fradet-Turcotte *et al*, 2013; Callen *et al*, 2020). Although we did not investigate the mechanism by which NHEJ efficiency was decreased by GAPDH knockdown in detail in this study, HDAC1 might be the molecule mediating this process, in addition to the role it plays in as HR, because it plays a vital role in NHEJ repair by deacetylating H3K56 and affecting the aggregation of Ku70 at damage sites (Miller *et al*, 2010).

We identified a direct interaction between HDAC1 and GAPDH, and this interaction was enhanced after IR treatment. In addition, we discovered that HDAC1 activity was significantly decreased in GAPDH knockdown cells, suggesting that GAPDH positively regulated HDAC1 activity. However, HDAC1 activity was unexpectedly decreased when GAPDH was overexpressed. This effect might be related to cell apoptosis because overexpression of GAPDH induces cell apoptosis through cytochrome c release into the cytosol and nuclear translocation of apoptosis-inducing factor (Colell *et al*, 2007). HDAC1 activity has been revealed to be inhibited by Maspin binding (Li *et al*, 2006). Therefore, we examined Maspin protein levels and found no significant difference before and after GAPDH knockdown, excluding the possibility that the increase in Maspin inhibited HDAC1 activity. Interestingly, we found competitive HDAC1 binding with GAPDH and Maspin, which may explain the regulatory effect of GAPDH on HDAC1 activity. A similar mechanism was found in Chang's study, in which GAPDH activated SIRT1 under starvation conditions by interacting with SIRT1, displacing the SIRT1 suppressor (Chang *et al*, 2015). We wondered whether SIRT1 mediates the GAPDH knockdown-induced RAD51 decrease similar to HDAC1, and the hypothesis was clearly rejected by the result; overexpression of SIRT1 did not reverse RAD51 protein level reduction, suggesting that GAPDH activates different deacetylases depending on the type of stress involved. Notably, although GAPDH positively regulates HDAC1 activity, the latter was significantly decreased after IR exposure. Several reasons may explain this intriguing result. First, only a small portion of GAPDH is translocated into the nucleus. Second, the IR-decreased glycolytic activity of GAPDH may be critical for reduced HDAC1 activity. Third, other factors may be involved.

RAD51 is the key protein in HR, and its expression is regulated at different levels. Acetylation is a crucial post-translational modification of RAD51, affecting its expression; this effect was realized when HDAC inhibitors (HDACi), such as PCI-24781, TSA, and VPA, were shown to decrease the RAD51 protein level (Adimoolam *et al*, 2007; Liu *et al*, 2021; Romeo *et al*, 2022). Consistent with these results, our data showed that acetylation promotes the ubiquitinated degradation of RAD51. Previous literature has shown that deubiquitination promotes the binding of RAD51 to BRCA2 and facilitates RAD51 accumulation at DSB sites (Luo *et al*, 2016). Conversely, ubiquitination plays a critical role in the timely removal of RAD51 from DNA damage sites, enabling progression to the late phase of HR (Inano *et al*, 2017). Therefore, these findings suggest that acetylation-dependent ubiquitination of RAD51 may be significant for its function at different stages of HR. Further investigation is needed to explore this issue in the future. Furthermore, we applied an LC–MS/MS assay to analyze acetylated recombinant RAD51 and identified several acetylated lysine residues. Among these sites, Lys40 is essential for RAD51 protein stability, and an evolutionary

conservation analysis and the effect of mutations of this site suggest its importance. Since acetylation is the result of a balance between acetylase and deacetylase, the decrease of RAD51 protein levels after GAPDH knockdown can be explained, on the one hand, by the reduction of HDAC1 activity that we had detected and, on the other hand, by the result of an increase in acetylase activity, as indicated by Sen *et al* (2008), who reported that nitric oxide-induced nuclear GAPDH activated p300/CBP. Therefore, further investigation is needed to determine whether p300/CBP is involved in this process. Moreover, acetylated modification of RAD51 may follow a time-dependent pattern, which may better explain its timely elimination during the HR process. It is noteworthy that in addition to acetylase and deacetylase, several other factors have been identified as regulators of RAD51 protein levels, such as β1-integrin (Ahmed *et al*, 2018), RFWD3 (Inano *et al*, 2017), and MDC1 (Xiong *et al*, 2015). These factors collectively contribute to the equilibrium that keeps the intracellular RAD51 level constant in the absence of DSBs. However, when this equilibrium is disrupted, or cells are exposed to DSB-inducing agents, the RAD51 level is impacted. Therefore, the observed partial decrease in RAD51 levels in GAPDH knockdown cells may be attributed to multiple factors, which include the acetylation-dependent ubiquitination of RAD51 regulated by GAPDH, as well as the influence of various other factors.

In conclusion, our study revealed that GAPDH regulates RAD51 acetylation and stability by binding with HDAC1 and enhancing its activity, which highlights the importance of GAPDH in HR repair. Since IR resistance in human cancers has been linked to enhanced HR repair, these findings may establish a rationale for the development of GAPDH-targeted approaches for cancer treatment.

Materials and Methods

Cell culture and reagents

The human cervical cancer cell line HeLa cells, human embryonic kidney cell line HEK293T, and BEAS-2B cell line were purchased from ATCC; U2OS cells containing NHEJ reporter system and HRR reporter system, and pCAGGS-I-SceI plasmid were gifts from Liu Songbai's group at Suzhou Vocational Health College. HK2 cell line was gift from Xu Qian's group at Nanjing Medical University. These cells were cultured in Dulbecco's modified eagle's (DMEM) or RPMI-1640 (Keygen Biotech, China) supplemented with 10% fetal bovine serum (Biochannel, China) and 1% penicillin and streptomycin (Solarbio, Beijing, China). For stable knockdown GAPDH HeLa cells, the cell was infected with specific lentivirus vectors for 48 h and then selected with puromycin (Solarbio, China) for 3 weeks. Cycloheximide (S7418), camptothecin (S1228), adriamycin (S1208), and etoposide (S1225) were purchased from Selleckche. MG132 (HY-13259), Trichostatin A (HY-15144), and PP2 (HY-13805) were obtained from MedChem Express. Heptelidic acid (GC43816) was purchased from GLPBIO. The recombinant HDAC1 (IICH8936) and Maspin (ICH8931) were purchased from ImmunoClone.

Antibodies

The antibodies used for immunoblot, immunoprecipitation, and immunofluorescence analysis are listed in Appendix Table S1.

Plasmid constructs and transfection

Flag-tagged GAPDH, Flag-tagged GAPDH-Y41F, and Flag-tagged HDAC1 in pFLAG-CMV4 have been described previously (Ci *et al*, 2020). Flag-tagged RAD51 and SIRT1 cloned into p-ENTER plasmid were purchased from Vigene Biosciences (China). The K40/64/70/80/285R of RAD51 in p-ENTER, S122A/S122D and C152S mutants of GAPDH and H141A of HDAC1 in pFLAG-CMV4 were generated by 2× Phanta Flash Master Mix (Vazyme, China) using primers listed in Appendix Table S2. Flag-tagged HDAC1 truncated mutations were generated by cloning the corresponding HDAC1 sequence into a pFLAG-CMV4 vector at *Eco*R I and *Kpn* I sites. 6× His-tagged RAD51 was generated by cloning the corresponding RAD51 sequence into a pET-28a vector at *Bam*H I and *Hind* III sites. All constructs were verified by sequencing. The lentivirus vectors were constructed and purified by Corues Biotechnology Company (China) for the knockdown of GAPDH. The shRNA sequences are described in Appendix Table S2. According to the manufacturer's instructions, indicated plasmids were transfected using ExFect Transfection Reagent (Vazyme, China).

Western blot

Cells were washed with PBS three times and lysed in RIPA buffer. The proteins were separated using 12% SDS–PAGE and transferred onto PVDF membranes (Roche, Switzerland). After blocking in PBS with 5% skim milk for 1.5 h, the membranes were incubated with the corresponding primary antibodies overnight at 4°C. After washing the membrane three times for 5 min each time with PBST, incubate the secondary antibody for 1 h at room temperature, and then wash the membrane 3 times with PBST. The chemiluminescence solution was prepared according to the instructions and added to the PVDF membrane in drops. The images were scanned by Tanon 4500 Imaging System (China) and quantified with ImageJ (National Institutes of Health, USA).

Reverse transcription and quantitative real-time PCR

Total RNA was isolated from cells using Trizol reagent following the manufacturer's protocol (Invitrogen, USA). Total RNAs of 0.5–1 μg were used as templates for the reverse transcription using HiScript Q RT SuperMix for qPCR (Vazyme, China). Quantitative PCR (qPCR) was conducted using ChamQ SYBR qPCR Master Mix (High ROX Premixed) according to the manufacturer's protocol (Vazyme, China). The primers for human GAPDH, RAD51, HDAC1, and Actin are described in Appendix Table S2.

Immunoprecipitation

Cells were washed with PBS three times and then lysed using IP lysis buffer (Beyotime Biotechnology, China) supplemented with PMSF and cocktail (Roche, Switzerland). The lysates were incubated on a 4°C rotator for 3 h. A 10% aliquot of supernatant was saved as input. The remaining supernatant was treated with 100 μg/ml DNase I for 15 min and divided into two tubes. One tube was incubated with the corresponding antibody-conjugated protein A/G magnetic beads (Bimake, USA) or anti-Flag M2 beads (Sigma-Aldrich, Germany), while the other tube served as

a control and was incubated with control IgG antibody. The protein-bead complexes were washed three times with PBS containing PMSF and cocktail to remove nonspecifically bound proteins and contaminants. The proteins were detected using immunoblot. For *in vitro* immunoprecipitation, purified His-tagged GAPDH proteins were incubated with recombinant HDAC1 and Maspin at 37°C for 2 h; HDAC1 antibody was added to the mixture in IP lysis buffer, followed by further incubation at 4°C overnight. Protein A/G magnetic bead was used for immunoprecipitation. Separated proteins were applied for immunoblotting afterward.

Immunofluorescence

Cells were washed with PBS three times and fixed with 4% paraformaldehyde for 10 min, permeabilized with 0.1–0.5% Triton X-100 for 10 min, and blocked with 3% BSA for 1 h at room temperature. After blocking, cells were incubated with indicated primary antibodies overnight at 4°C. Subsequently, cells were washed with PBST and incubated with fluorescent secondary antibodies for 2 h at room temperature. Next, cells were stained with DAPI and visualized by fluorescence microscope (80I 10-1500X; Nikon, Japan), and the images were captured with a charge-coupled device camera.

Comet assay

For neutral comet assay, cells were harvested at various times post-IR and mixed with low melting point agarose gel onto the Comet Slide. Transfer the slide to a small basin/container containing a prechilled Neutral Lysis Storage Buffer (Tris 10 mM, NaCl 2.5 M, Na_2EDTA 30 mM, pH = 10) for 2 h in 4°C. Aspirate the Lysis Buffer and replace it with prechilled Neutral Lysis Working Buffer (Neutral Lysis Storage Buffer 89 ml, TritonX-100 1 ml, DMSO 9 ml). Immerse the slide in the solution for 30 min at 4°C in the dark. Fill the chamber with cold Neutral Electrophoresis Solution (Tris 100 mM, CH_3COONa 300 mM, pH = 9) and apply voltage to the chamber for 30 min at 25 volt. Add 10 μl/well of diluted PI till the agarose and slide is completely dry. Incubate at room temperature for 15 min. Each slide was photographed under a Zeiss Axiovert 200M microscope, and comet tail analysis was computed by the ImageJ using the OpenComet plugin.

For the Alkaline Comet assay, cells were harvested at various times post-IR and processed for neutral comet assay using a DNA Damage Detection Kit (KeyGEN BioTECH, China), according to the manufacturer's protocol.

In vitro acetylation assay and mass spectrometric analysis

His-tagged RAD51 was purified by His-tagged Protein Purification Kit as the manufacturer's procedure (CoWin Biosciences, China). In 50 μl reaction buffer containing His-tagged RAD51 5 μg, 8 μg HeLa cell lysate as acetyltransferase donor, 50 μM Tris–HCL (pH = 8.0), 20 μM acetyl-CoA, 0.1 mM EDTA, 1 mM DTT, and 10% Glycerol was constructed and incubated at 37°C for 1 h. Then, the samples were divided into two aliquots for immunoblot, and Coomassie dyed the gel. The proteins in gel bands were excised and then sent to Oebiotech for mass spectrometric analysis.

HDAC1 activity assay

Cell subcellular fractions were separated by following the manufacturer's protocol of Nuclear and Cytoplasmic Extraction Kit (Cowin Biosciences, China). For *in vitro* HDAC1 activity assay, purified His-tagged GAPDH proteins were incubated with 50 μg nucleoproteins at 37°C for 15 min, and then HDAC1 activity was measured using an HDAC1 assay kit (HALING Biological Technology Co., LTD, China) following the manufacturer's protocol.

GAPDH activity assay

GAPDH enzymatic activity was determined by GAPDH Assay Kit (HALING Biological Technology Co., LTD, China) following the manufacturer's instructions. HeLa cells were treated as indicated, then washed three times with PBS and lysed with lysis buffer. The experiments were carried out according to the instructions that the total GAPDH activity is quantified by measuring the change in absorbance (340 nm wavelength).

Intracellular ROS production assays

Intracellular ROS production was measured by ROS Assay Kit (Beyotime, Shanghai, China). HeLa cells were subjected to the indicated treatments, followed by incubation with 10 mM DCFH-DA in fresh medium at 37°C for 30 min. The cells were washed three times with PBS and lysed in lysis buffer (50% methanol with 0.1 M NaOH). After gently detaching the cells from the plate and centrifuging at 4500 rpm for 5 min, the resulting supernatants were analyzed for fluorescence at 488/525 nm using a flow cytometer (BD Biosciences, USA).

Cell survival assay

Cell survival was measured by Cell Counting Kit-8 (APExBIO, USA). Cells were seeded onto a 96-well plate in 100 μl cell culture medium of each well. After treatment with the indicated concentrations of ADR, add 10 μl CCK-8 solution to each well of the plate. Then, incubate the plate for 1.5 h in the incubator and measure the absorbance at 450 nm using a microplate reader (TECAN infinite F200 PRO, Switzerland).

HR efficiency assay

DR-GFP U2OS cells were seeded in 6-well plate and transfected with scramble siRNA and GAPDH siRNA for 12 h and then transfected with pCAGGS-I-SceI plasmid. After 24 h, cells were harvested for GFP expression detection by flow cytometry (BD Biosciences, USA).

Cell cycle

After being transfected with indicated siRNA or treated with indicated drugs, cells were collected and fixed in cold 70% ethanol at −20°C for 12 h, and then cells were stained with propidium iodide (PI) for 30 min at 37°C. At least 10,000 cells were analyzed by FACS (BD Biosciences, USA). Data were analyzed by ModFit LT.

Statistical analysis

The numerical data obtained from the experiments were compared between two groups using GraphPad Prism 8.0. The appropriate statistical tests, such as *t*-test, ANOVA, or Mann–Whitney *U*-test, were performed to determine the significance, with $P < 0.05$ representing a significant difference between the groups and ns representing not significant. The image data were processed and analyzed using Photoshop and Image J, and the data were statistically analyzed using GraphPad Prism. All experimental data were obtained from three independent experiments.

Data availability

Our study includes no data deposited in public repositories.

Expanded View for this article is available online.

Acknowledgements
The authors thank Dr. Songbai Liu (Suzhou Vocational Health College, Suzhou, China) for providing the U2OS EJ5-GFP cell line and the U2OS DR-EGFP cell line, and Dr. Xu Qian (Nanjing Medical University) for his kind gift of HK2 (human kidney 2) cell line. This work was supported by the National Natural Science Foundation of China (grants 81872284, 82002548), the Natural Science Research of Jiangsu Higher Education Institutions of China (grant 18KJA180006), and the Postgraduate Research & Practice Innovation Program of Jiangsu Province (grant KYCX21_1370).

Author contributions
Munan Shi: Conceptualization; resources; data curation; software; formal analysis; funding acquisition; validation; investigation; visualization; methodology; writing – original draft; writing – review and editing. **Jiajia Hou:** Conceptualization; resources; data curation; software; formal analysis; investigation; visualization; methodology; writing – review and editing. **Weichu Liang:** Conceptualization; resources; data curation; software; formal analysis; validation; investigation; visualization; methodology; writing – original draft. **Qianwen Li:** Resources; methodology. **Shan Shao:** Data curation; validation; visualization. **Shusheng Ci:** Investigation; methodology. **Chuanjun Shu:** Visualization. **Xingqi Zhao:** Investigation; methodology. **Shanmeizi Zhao:** Resources; investigation; methodology. **Miaoling Huang:** Investigation; methodology. **Congye Wu:** Funding acquisition. **Zhigang Hu:** Supervision. **Lingfeng He:** Supervision. **Zhigang Guo:** Conceptualization; resources; supervision; funding acquisition; project administration; writing – review and editing. **Feiyan Pan:** Conceptualization; resources; supervision; funding acquisition; writing – original draft; writing – review and editing.

Disclosure and competing interests statement
The authors declare that they have no conflict of interest.

References

Adimoolam S, Sirisawad M, Chen J, Thiemann P, Ford JM, Buggy JJ (2007) HDAC inhibitor PCI-24781 decreases RAD51 expression and inhibits homologous recombination. *Proc Natl Acad Sci USA* 104: 19482 – 19487

Ahmed KM, Pandita RK, Singh DK, Hunt CR, Pandita TK (2018) beta1-integrin impacts Rad51 stability and DNA double-strand break repair by homologous recombination. *Mol Cell Biol* 38: e00672-17

Azam S, Jouvet N, Jilani A, Vongsamphanh R, Yang X, Yang S, Ramotar D (2008) Human glyceraldehyde-3-phosphate dehydrogenase plays a direct role in reactivating oxidized forms of the DNA repair enzyme APE1. *J Biol Chem* 283: 30632 – 30641

Callen E, Zong D, Wu W, Wong N, Stanlie A, Ishikawa M, Pavani R, Dumitrache LC, Byrum AK, Mendez-Dorantes C *et al* (2020) 53BP1 enforces distinct pre- and post-resection blocks on homologous recombination. *Mol Cell* 77: 26 – 38.e7

Chakravarti R, Aulak KS, Fox PL, Stuehr DJ (2010) GAPDH regulates cellular heme insertion into inducible nitric oxide synthase. *Proc Natl Acad Sci USA* 107: 18004 – 18009

Chang C, Su H, Zhang D, Wang Y, Shen Q, Liu B, Huang R, Zhou T, Peng C, Wong CC *et al* (2015) AMPK-dependent phosphorylation of GAPDH triggers Sirt1 activation and is necessary for autophagy upon glucose starvation. *Mol Cell* 60: 930 – 940

Chen CC, Feng W, Lim PX, Kass EM, Jasin M (2018) Homology-directed repair and the role of BRCA1, BRCA2, and related proteins in genome integrity and cancer. *Annu Rev Cancer Biol* 2: 313 – 336

Ci S, Xia W, Liang W, Qin L, Zhang Y, Dianov GL, Wang M, Zhao X, Wu C, Alagamuthu KK *et al* (2020) Src-mediated phosphorylation of GAPDH regulates its nuclear localization and cellular response to DNA damage. *FASEB J* 34: 10443 – 10461

Ciccia A, Elledge SJ (2010) The DNA damage response: making it safe to play with knives. *Mol Cell* 40: 179 – 204

Clarke TL, Sanchez-Bailon MP, Chiang K, Reynolds JJ, Herrero-Ruiz J, Bandeiras TM, Matias PM, Maslen SL, Skehel JM, Stewart GS *et al* (2017) PRMT5-dependent methylation of the TIP60 coactivator RUVBL1 is a key regulator of homologous recombination. *Mol Cell* 65: 900 – 916.e7

Colell A, Ricci JE, Tait S, Milasta S, Maurer U, Bouchier-Hayes L, Fitzgerald P, Guio-Carrion A, Waterhouse NJ, Li CW *et al* (2007) GAPDH and autophagy preserve survival after apoptotic cytochrome *c* release in the absence of caspase activation. *Cell* 129: 983 – 997

Dar GH, Mendes CC, Kuan WL, Speciale AA, Conceicao M, Gorgens A, Uliyakina I, Lobo MJ, Lim WF, El Andaloussi S *et al* (2021) GAPDH controls extracellular vesicle biogenesis and enhances the therapeutic potential of EV mediated siRNA delivery to the brain. *Nat Commun* 12: 6666

Demarse NA, Ponnusamy S, Spicer EK, Apohan E, Baatz JE, Ogretmen B, Davies C (2009) Direct binding of glyceraldehyde 3-phosphate dehydrogenase to telomeric DNA protects telomeres against chemotherapy-induced rapid degradation. *J Mol Biol* 394: 789 – 803

Fradet-Turcotte A, Canny MD, Escribano-Diaz C, Orthwein A, Leung CCY, Huang H, Landry M-C, Kitevski-LeBlanc J, Noordermeer SM, Sicheri F *et al* (2013) 53BP1 is a reader of the DNA-damage-induced H2A Lys 15 ubiquitin mark. *Nature* 499: 50 – 54

Galvan-Pena S, Carroll RG, Newman C, Hinchy EC, Palsson-McDermott E, Robinson EK, Covarrubias S, Nadin A, James AM, Haneklaus M *et al* (2019) Malonylation of GAPDH is an inflammatory signal in macrophages. *Nat Commun* 10: 338

Hara MR, Agrawal N, Kim SF, Cascio MB, Fujimuro M, Ozeki Y, Takahashi M, Cheah JH, Tankou SK, Hester LD *et al* (2005) S-nitrosylated GAPDH initiates apoptotic cell death by nuclear translocation following Siah1 binding. *Nat Cell Biol* 7: 665 – 674

Harada N, Yasunaga R, Higashimura Y, Yamaji R, Fujimoto K, Moss J, Inui H, Nakano Y (2007) Glyceraldehyde-3-phosphate dehydrogenase enhances

transcriptional activity of androgen receptor in prostate cancer cells. *J Biol Chem* 282: 22651 – 22661

Hou X, Snarski P, Higashi Y, Yoshida T, Jurkevich A, Delafontaine P, Sukhanov S (2017) Nuclear complex of glyceraldehyde-3-phosphate dehydrogenase and DNA repair enzyme apurinic/apyrimidinic endonuclease I protect smooth muscle cells against oxidant-induced cell death. *FASEB J* 31: 3179 – 3192

Hustedt N, Durocher D (2016) The control of DNA repair by the cell cycle. *Nat Cell Biol* 19: 1 – 9

Inano S, Sato K, Katsuki Y, Kobayashi W, Tanaka H, Nakajima K, Nakada S, Miyoshi H, Knies K, Takaori-Kondo A *et al* (2017) RFWD3-mediated ubiquitination promotes timely removal of both RPA and RAD51 from DNA damage sites to facilitate homologous recombination. *Mol Cell* 66: 622 – 634

Ito A, Kawaguchi Y, Lai CH, Kovacs JJ, Higashimoto Y, Appella E, Yao TP (2002) MDM2-HDAC1-mediated deacetylation of p53 is required for its degradation. *EMBO J* 21: 6236 – 6245

Kornberg MD, Sen N, Hara MR, Juluri KR, Nguyen JV, Snowman AM, Law L, Hester LD, Snyder SH (2010) GAPDH mediates nitrosylation of nuclear proteins. *Nat Cell Biol* 12: 1094 – 1100

Kornberg MD, Bhargava P, Kim PM, Putluri V, Snowman AM, Putluri N, Calabresi PA, Snyder SH (2018) Dimethyl fumarate targets GAPDH and aerobic glycolysis to modulate immunity. *Science* 360: 449 – 453

Kosova AA, Khodyreva SN, Lavrik OI (2015) Glyceraldehyde-3-phosphate dehydrogenase (GAPDH) interacts with apurinic/apyrimidinic sites in DNA. *Mutat Res* 779: 46 – 57

Krejci L, Altmannova V, Spirek M, Zhao X (2012) Homologous recombination and its regulation. *Nucleic Acids Res* 40: 5795 – 5818

Li X, Heyer WD (2008) Homologous recombination in DNA repair and DNA damage tolerance. *Cell Res* 18: 99 – 113

Li X, Yin S, Meng Y, Sakr W, Sheng S (2006) Endogenous inhibition of histone deacetylase 1 by tumor-suppressive maspin. *Cancer Res* 66: 9323 – 9329

Liberti MV, Dai Z, Wardell SE, Baccile JA, Liu X, Gao X, Baldi R, Mehrmohamadi M, Johnson MO, Madhukar NS *et al* (2017) A predictive model for selective targeting of the Warburg effect through GAPDH inhibition with a natural product. *Cell Metab* 26: 648 – 659.e8

Liu G, Lim D, Cai Z, Ding W, Tian Z, Dong C, Zhang F, Guo G, Wang X, Zhou P *et al* (2021) The valproate mediates radio-bidirectional regulation through RFWD3-dependent ubiquitination on Rad51. *Front Oncol* 11: 646256

Luo K, Li L, Li Y, Wu C, Yin Y, Chen Y, Deng M, Nowsheen S, Yuan J, Lou Z (2016) A phosphorylation-deubiquitination cascade regulates the BRCA2-RAD51 axis in homologous recombination. *Genes Dev* 30: 2581 – 2595

Mal A, Sturniolo M, Schiltz RL, Ghosh MK, Harter ML (2001) A role for histone deacetylase HDAC1 in modulating the transcriptional activity of MyoD: inhibition of the myogenic program. *EMBO J* 20: 1739 – 1753

Martinez-Reyes I, Chandel NS (2021) Cancer metabolism: looking forward. *Nat Rev Cancer* 21: 669 – 680

Miller KM, Tjeertes JV, Coates J, Legube G, Polo SE, Britton S, Jackson SP (2010) Human HDAC1 and HDAC2 function in the DNA-damage response to promote DNA nonhomologous end-joining. *Nat Struct Mol Biol* 17: 1144 – 1151

Nakajima H, Kubo T, Ihara H, Hikida T, Danjo T, Nakatsuji M, Shahani N, Itakura M, Ono Y, Azuma YT *et al* (2015) Nuclear-translocated Glyceraldehyde-3-phosphate dehydrogenase promotes poly(ADP-ribose) Polymerase-1 activation during oxidative/nitrosative stress in stroke. *J Biol Chem* 290: 14493 – 14503

Nakajima H, Itakura M, Kubo T, Kaneshige A, Harada N, Izawa T, Azuma YT, Kuwamura M, Yamaji R, Takeuchi T (2017) Glyceraldehyde-3-phosphate dehydrogenase (GAPDH) aggregation causes mitochondrial dysfunction during oxidative stress-induced cell death. *J Biol Chem* 292: 4727 – 4742

Phadke MS, Krynetskaia NF, Mishra AK, Krynetskiy E (2009) Glyceraldehyde 3-phosphate dehydrogenase depletion induces cell cycle arrest and resistance to antimetabolites in human carcinoma cell lines. *J Pharmacol Exp Ther* 331: 77 – 86

Romeo MA, Gilardini Montani MS, Benedetti R, Arena A, D'Orazi G, Cirone M (2022) VPA and TSA interrupt the interplay between mutp53 and HSP70, leading to CHK1 and RAD51 Down-regulation and sensitizing pancreatic cancer cells to AZD2461 PARP inhibitor. *Int J Mol Sci* 23: 2268

San Filippo J, Sung P, Klein H (2008) Mechanism of eukaryotic homologous recombination. *Annu Rev Biochem* 77: 229 – 257

Sanchez-Bailon MP, Choi SY, Dufficy ER, Sharma K, McNee GS, Gunnell E, Chiang K, Sahay D, Maslen S, Stewart GS *et al* (2021) Arginine methylation and ubiquitylation crosstalk controls DNA end-resection and homologous recombination repair. *Nat Commun* 12: 6313

Sawa A, Khan AA, Hester LD, Snyder SH (1997) Glyceraldehyde-3-phosphate dehydrogenase: nuclear translocation participates in neuronal and nonneuronal cell death. *Proc Natl Acad Sci USA* 94: 11669 – 11674

Sen N, Hara MR, Kornberg MD, Cascio MB, Bae B-I, Shahani N, Thomas B, Dawson TM, Dawson VL, Snyder SH *et al* (2008) Nitric oxide-induced nuclear GAPDH activates p300/CBP and mediates apoptosis. *Nat Cell Biol* 10: 866 – 873

Shankar E, Pandey M, Verma S, Abbas A, Candamo M, Kanwal R, Shukla S, MacLennan GT, Gupta S (2020) Role of class I histone deacetylases in the regulation of maspin expression in prostate cancer. *Mol Carcinog* 59: 955 – 966

Srinivas US, Tan BWQ, Vellayappan BA, Jeyasekharan AD (2019) ROS and the DNA damage response in cancer. *Redox Biol* 25: 101084

Verdin E, Ott M (2015) 50 years of protein acetylation: from gene regulation to epigenetics, metabolism and beyond. *Nat Rev Mol Cell Biol* 16: 258 – 264

Wu Y, Wu M, He G, Zhang X, Li W, Gao Y, Li Z, Wang Z, Zhang C (2012) Glyceraldehyde-3-phosphate dehydrogenase: a universal internal control for Western blots in prokaryotic and eukaryotic cells. *Anal Biochem* 423: 15 – 22

Xiong X, Du Z, Wang Y, Feng Z, Fan P, Yan C, Willers H, Zhang J (2015) 53BP1 promotes microhomology-mediated end-joining in G1-phase cells. *Nucleic Acids Res* 43: 1659 – 1670

Zeng T, Dong ZF, Liu SJ, Wan RP, Tang LJ, Liu T, Zhao QH, Shi YW, Yi YH, Liao WP *et al* (2014) A novel variant in the 3' UTR of human SCN1A gene from a patient with Dravet syndrome decreases mRNA stability mediated by GAPDH's binding. *Hum Genet* 133: 801 – 811

Zhu X, Jin C, Pan Q, Hu X (2021) Determining the quantitative relationship between glycolysis and GAPDH in cancer cells exhibiting Warburg effect. *J Biol Chem* 296: 100369